Inorganica Chimica Acta, 43 (1980) 49–58
©Elsevier Sequoia S.A., Lausanne – Printed in Switzerland

Multi-step Kinetics of Aquo Aluminum(III)–Ferron (8-Hydroxy-7-Iodo-5-Quinoline) Complexation Reactions

J. H. FERGUSON[‡], K. KUSTIN*
Department of Chemistry, Brandeis University, Waltham, Mass. 02254, U.S.A.

and A. PHIPPS
Gillette Company, Gillette Park T-2, Boston, Mass. 02106, U.S.A.

Received April 21, 1980

The interaction of excess hydrolyzed aluminum(III) cation in mildly acid aqueous media with ferron (7-iodo-8-hydroxyquinoline-5-sulfonic acid) has been studied using stopped-flow. Three distinct transients are observed. The shortest-lived, which is largest in amplitude, has been assigned to mono-complex formation. The other two transients, which are much smaller in amplitude, are interpreted as reactions of dimeric and other polymeric aluminum(III) species.

The hydrogen ion dependences of the observed rate constants for mono-complex formation indicate participation of $Al(OH)_2^+$ in the dominant pathway. Analysis of these results, using the Eigen model of complexation, leads to a water exchange rate constant of $(4.0 \pm 0.4) \times 10^7$ sec^{-1} for $Al(OH)_2^+$.

The slower transients could not be adequately explained by formation of bis- and tris-complexes. Assignment of these transients to reactions of μ-hydroxy-bridged aluminum dimer with ferron, coupled to mono-complex formation leads to an adequate data fit. The polyphasic nature of the aluminum–ferron interaction over the pH range 2–5 can be understood as showing different groups of reactions, rather than differently reacting metal-containing species.

Introduction

Complexes of mono- and divalent metal ions form rapidly in aqueous solution [1]. Formation of a complex is pictured as the substitution of coordinated water molecules by the incoming ligand. Mechanistically, the process is usually dissociative; the rate-determining step is rupture of the metal–water bond. Tervalent ions, however, may substitute associatively as well as dissociatively as exemplified by iron(III) complexation [2].

Interactions between aluminum(III) and complexing ligands are especially difficult to unravel because of this metal ion's pronounced tendency to hydrolize and polymerize [3]. Early work on the kinetics of aluminum(III) complexation concentrated on inorganic sulfate as ligand [4], but more recently reactions with organic ligands have been investigated [5–7]. These studies yield substitution rate constants for Al^{3+} consistent with the lifetime of a coordinated water molecule [8], and show that $AlOH^{2+}$ is a more reactive species.

Speciation in aluminum solutions is not straightforward, however; there are many more than two aluminum ions in dilute acid solution [9]. This situation is shown strikingly when the ligand ferron (8-hydroxy-7-iodo-5-quinolinesulfonic acid) is added to solutions of aluminum(III); for the development of the colored Al(III)–ferron complexes takes place over a relatively long period of time (24 hrs), in at least three discrete stages [3, 10–12]. This kinetic behavior has been interpreted as arising from reactions of monomeric Al (<1 sec.), oligomeric Al (~30 min.), and polymeric Al (~24 hrs.) [10, 11]. No kinetics data had been collected for the fastest (<1 sec.) interaction upon which to base this assignment. Consequently, we are reporting a stopped-flow study of aluminum(III) complexation by ferron, to determine which species participate in the fastest observed reaction.

Experimental

Materials

All reagent grade chemicals, used without further purification, were supplied by Fisher Scientific Co. except for aluminum perchlorate ($Al(ClO_4)_3 \cdot 9H_2O$,

---

*Author to whom all correspondence should be addressed.

[‡] Present address: Polaroid Corporation, 1 Upland Road N-2, Norwood, Mass. 02062, U.S.A.

Atomeric Chemical Co.) and 8-hydroxy-7-iodo-5-quinoline sulfonic acid (ferron, m.p. 260 °C, City Chemical Corp.). Doubly distilled water from an all glass still was used for all solutions.

Kinetics Studies

All kinetics studies were done on a stopped-flow spectrophotometer with the photomultiplier output voltage recorded by a Biomation 610B transient recorder. This recorder had been modified with an optional X100 multiplier circuit on the last six sample time positions extending the elapsed time of the 255 point data set to a maximum of 21.25 min. The voltage *versus* time data set was then digitalized and output onto a magnetic cassette tape of a Texas Instruments 733 terminal at 1200 baud by a Pivan Datacap B103 interface.

Data analysis was done on a DEC PDP 10 computer using an approach-to-equilibrium least squares method. For runs showing two coupled but separable relaxations a 'peeling-off' technique was used [13]. Standard linear and non-linear least squares methods were used for further analysis. For a given set of reactant concentrations at least six (for the constant metal–pH variation study) but in most cases twelve (for the metal-pH variation study) runs were recorded, analyzed and averaged. The observed rate constants found in this manner had relative internal errors (deviation from pseudo-first-order rate equation) of between 0.8–1.3% for the 'fast' effect and less than 3% for the 'slow' effect. Relative deviation from the mean for the averaged runs was less than 5% for the 'fast' effect and 10% for the 'slow' effect.

Throughout these studies the reaction was monitored at 370 nm while the temperature was held at 25.0 ± 0.1 °C by a Forma-termp Jr. water bath Ionic strength was held constant at 1 *M* by addition of appropriate sodium salts as needed. The aluminum concentration was in pseudo-first-order excess (at least 25 fold) of the ferron concentration. Ligand solutions were made by dilution of a stock solution which was replaced at least every two weeks but which showed no signs of decomposition within that period. Aluminum stock solutions were prepared by weight and, unless otherwise noted, the pH adjusted by careful addition of dilute sodium hydroxide to the rapidly stirred solution so that little if any transient precipitate formed. The solutions were then allowed to stand a minimum of ten days before the pH was measured and dilutions made.

pH Measurement

An Orion 801A pH/mv meter with an Orion 91-03 combination electrode was used to make pH measurements. The aluminum solutions tend to coat the electrode membrane, however, causing high readings. In order to compensate for this effect the electrode was calibrated using Fisher Gram-Pac buffer and then immersed in the aluminum stock solution. The pH reading slowly increased and stabilized at a value approximately 0.3 pH units higher than the initial reading. The 'poisoned' electrode was then used to measure a set of aluminum stock solutions with different pH's until a stable reading was obtained for each. Upon reimmersion in the buffer the apparent pH was recorded; within 10–15 minutes the electrode reading had returned to the actual value of the buffer. This masking effect appears to be linear in pH as very similar displacements are found with both solutions of different pH and with different buffers. By compensating for this masking a set of relative pH's was obtained to within ±0.01 pH units.

Dilutions of the aluminum stock solution were made into 1 *M* ionic strength solutions of the appropriate sodium salt which had been adjusted to the proper pH. Dilution caused no significant change in pH within the concentration set.

In the first studies we undertook, such as the anion-variation and the constant metal-pH variation studies, this procedure for pH measurement was not followed so that the pH values are high for these data. The corrections involved are dependent on the aluminum concentrations and on electrode conditions since the porous plug of the combination electrode also is affected by long term exposure to aluminum solutions.

All [H$^+$]'s were taken as antilog $(-\text{pH})/\gamma_\pm$ with $\gamma_\pm$ being the mean activity coefficient of the acid of the anion involved [14].

The equilibrium quotients used for data analysis (Table I) were corrected to 1 *M* ionic strength using log (Equilibrium Quotient) = log (Equilibrium Constant) + $aI^{1/2}/(1 + I^{1/2}) + bI$; with a, b being empirical constants found from measurement at various ionic strengths [15].

Results and Treatment of Data

General Observations

Representative oscilloscope traces of the Al(III)–ferron reaction are shown in Fig. 1, under the conditions of excess aluminum at pH 2.6. Of principal interest is the large, rapidly increasing absorbance change (1a) which is followed by two more slowly decreasing absorbance changes (1b, 1c). The magnitude of the second effect (1b) is about 2–5% that of the first (1a). Lowering the metal concentration causes the second effect, which is one of decreasing absorbance, to change to one of increasing absorbance (1d). The changeover occurs at lower metal concentration as the pH is raised. Quantitative data has been collected for the first two effects (1a, 1b or 1d), but not for the third (1c) since the time scale

TABLE I. Equilibrium Constants[a] Used in This Paper.

Aluminum hydrolysis and polymerization[b]		
K_{a1}^{M}	$= [AlOH^{+2}][H^+]/[Al^{+3}]$	$= 10^{-5.48}$ (M)
K_{a2}^{M}	$= [Al(OH)_2^+][H^+]/[AlOH^{+2}]$	$= 10^{-4.80}$ (M)
K_{a3}^{M}	$= [Al(OH)_3][H^+]/[Al(OH)_2^+]$	$= 10^{-5.80}$ (M)
$K_{21}^{M_2}$	$= [\mu\text{-}Al_2OH^{+5}][H^+]/[Al^{+3}]^2$	$= 10^{-4.17}$ (M)[c]
$K_{22}^{M_2}$	$= [\text{di-}\mu\text{-}Al_2(OH)_2^{+4}][H^+]^2/[Al^{+3}]^2$	$= 10^{-7.70}$ (M)[c]
$K_{34}^{M_3}$	$= [Al_3(OH)_4^{+5}][H^+]^4/[Al^{+3}]^3$	$= 10^{-13.47}$ (M)
$K_{13,24}^{M_{13}}$	$= [Al_{13}O_4(OH)_{24}^{+7}][H^+]^{32}/[Al^{+3}]^{13}$	$= 10^{-17.4}$ (M)
Ferron hydrolysis[d]		
$K_{a_1}^{L}$	$= [L^{-2}][H^+]/[HL^-]$	$= 10^{-7.27}$ (M)
K_{a2}^{L}	$= [HL^-][H^+]/[H_2L]$	$= 10^{-2.65}$ (M)
Aluminum–ferron complex stability[e]		
K_{11}^{ML}	$= [AlL^+]/[Al^{+3}][L^{-2}]$	$= 10^{+7.6}$ (M^{-1})
K_{12}^{ML}	$= [AlL_2^-]/[Al^{+3}][L^{-2}]^2$	$= 10^{+7.1}$ (M^{-1})
K_{13}^{ML}	$= [AlL_3^{-3}]/[Al^{+3}][L^{-2}]^3$	$= 10^{+5.6}$ (M^{-1})

[a] Ionic strength corrections were made in the manner of Baes and Mesmer, 'The Hydrolysis of Cations', Wiley-Interscience, New York (1976), p. 19. [b] Unless otherwise noted, the values listed in this section are based on Baes and Mesmer, *ibid.*, p. 121. [c] R. C. Turner, *Can. J. Chem.*, *53*, 2811 (1975). [d] Parallel to the treatment listed in fn. (a) using the values given for the ferron hydrolysis listed in L. G. Sillen and A. E. Martell, 'Stability Constants of Metal–Ion Complexes', Spec. Publ. 25, The Chemical Society, London, (1971), p. 596. [e] F. J. Langmyhr and A. R. Storm, *Acta Chem. Scand.*, *15*, 1461 (1961).

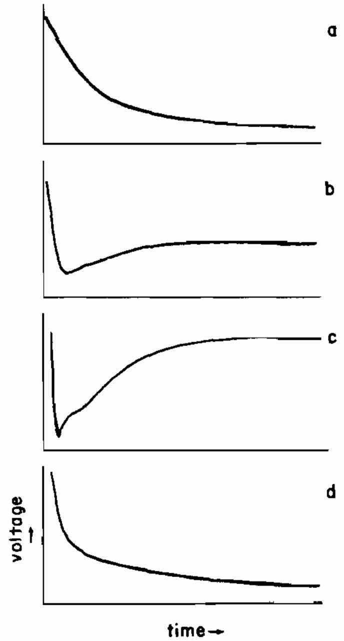

Fig. 1. Representative oscilloscope traces of the aluminum-(III)–ferron reaction. Vertical axis is photomultiplier voltage, which is proportional to the transmittance of the solution. A decrease in the voltage indicates an increase in the absorbance of the solution. Conditions: $[Al^{+3}] = 8.33 \times 10^{-2}$ M, [ferron] $= 1.45 \times 10^{-4}$ M, pH 2.60. (a) 0.5 volts full scale; 0.25 sec. elapsed time; (b) 0.05 volts full scale; 5 sec. elapsed time; (c) 0.05 volts full scale; 21 min. elapsed time; (d) $[Al^{+3}] = 4.16 \times 10^{-3}$ M; [ferron] $= 1.45 \times 10^{-4}$ M, pH 2.66, 0.2 volts full scale; 51 sec. elapsed time.

involved is only conveniently accessible at high metal concentration and high pH.

The age [11, 16, 17] and method of preparation [18] of an aluminum solution have a profound

TABLE II. Observed Rate Constants for the 'Fast' Effect of the Aluminum(III)-Cation–Ferron Reaction.

	$[Al^{+3}]_{total} \times 10^3$ (M) pH	0.416	0.833	1.67	3.33	4.99	6.66	8.33
					k^{obs} (sec^{-1})[a]			
ClO_4^- anion	2.57	–	–	0.28(0.02)	0.32(0.02)	0.72(0.01)	1.06(0.05)	1.36(0.11)
	2.72	–	0.26(0.01)	0.55(0.06)	2.00(0.02)	3.4(0.2)	4.6(0.2)	6.37(0.07)
	2.88	0.46(0.05)	0.91(0.03)	2.8(0.3)	7.4(0.7)	10.0(0.2)	13.7(0.5)	16.6(0.6)
	2.98	0.91(0.05)	3.4(0.2)	8.4(0.3)	17.1(1.1)	22.8(0.9)	26.6(1.0)	32.5(1.7)
	3.16	2.5(0.1)	7.8(0.3)	17.6(0.5)	29.2(0.8)	42.0(2.0)	51.0(2.2)	63.2(3.0)
	3.18	1.02(0.04)	3.1(0.7)	9.58(0.8)	22.8(1.5)	37.6(2.6)	46.8(1.8)	53.8(2.3)
Cl^- anion	2.68	–	–	0.36(0.05)	0.76(0.01)	1.10(0.05)	1.75(0.06)	2.11(0.12)
	2.76	–	0.45(0.01)	0.95(0.03)	2.6(0.1)	4.1(0.1)	5.98(0.08)	7.65(0.20)
	2.86	0.35(0.01)	0.95(0.02)	3.20(0.15)	7.6(0.3)	9.8(0.3)	12.9(0.3)	15.2(0.4)
	2.96	0.71(0.01)	2.1(0.1)	5.9(0.2)	11.8(0.4)	16.3(0.3)	18.8(0.4)	22.9(0.6)
	3.08	1.24(0.04)	4.2(0.2)	9.96(0.4)	17.7(0.2)	26.0(0.9)	34.4(1.5)	41.4(1.1)

[a] The number in the parenthesis for each entry is its associated standard deviation (±sigma).

TABLE III. Observed Rate Constants for the 'Slow' Effect of the Aluminum(III)-Cation–Ferron Reaction.

$[Al^{+3}]_{total} \times 10^3$ (*M*)		0.416	0.833	1.67	3.33	4.99	6.66	8.33
	pH				k^{obs} $(sec^{-1})^a$			
ClO_4^- anion	2.57	–	–	0.013(0.001)	–	0.065(0.01)	0.11(0.01)	0.12(0.01)
		2.6(0.2)[b]	4.5(0.5)	9.5(2.0)	3.7(0.2)	4.3(0.1)	–	–
	2.72	–	–	–	0.19(0.01)	0.31(0.02)	0.36(0.01)	0.37(0.02)
	2.88	–	–	0.31(0.06)	0.66(0.03)	0.90(0.04)	0.96(0.09)	1.23(0.06)
	2.98	0.22(0.03)	0.33(0.03)	0.75(0.04)	1.16(0.14)	1.29(0.12)	1.4(0.1)	1.5(0.1)
	3.16	0.22(0.02)	0.53(0.05)	0.62(0.02)	1.05(0.2)	–	–	2.03(0.3)
	3.18	0.39(0.12)	0.28(0.06)	1.04(0.16)	1.13(0.24)	1.26(0.09)	–	1.7(0.4)
Cl^- anion	2.68	–	–	0.22(0.02)	–	0.11(0.01)	0.19(0.03)	0.22(0.02)
	2.76	–	–	–	0.32(0.04)	0.52(0.04)	0.58(0.07)	0.69(0.05)
	2.86	0.014(0.001)	0.13(0.04)	–	–	–	–	1.27(0.09)
	2.96	–	0.27(0.03)	0.48(0.08)	0.76(0.15)	1.37(0.07)	1.38(0.15)	1.51(0.08)
	3.08	0.11(0.03)	0.29(0.04)	0.55(0.08)	0.95(0.1)	1.1(0.2)	1.1(0.3)	2.0(0.3)

[a] The number in parenthesis for each entry is its associated standard deviation (±sigma). [b] Value ×10^3 for a slower third effect on which no systematic study was carried out.

effect on the distribution of species present, with the system slowly equilibrating with time. At low aluminum concentrations the observed complexation reaction with freshly prepared solutions is very different from reaction with an aged solution. The magnitude of the 'slower' (1d) effect is much greater in the fresh solution causing a masking of the 'fast' effect (1a), leading to a separability problem. With aged solutions the 'slower' effect decreases in magnitude and becomes easily separable.

Metal Concentration and pH Dependences

'Fast' effect

Results of metal concentration, anion and pH variation studies for the 'fast' (1a) effect are listed in Table II. Plots of k^{obs} against total metal (Fig. 2) show a linear metal and an inverse hydrogen ion dependence. Superposition of the plots for perchlorate and chloride anion show that they are virtually identical, indicating that there is no significant interaction between the anion and reactants involved in the 'fast' effect.

'Slow' Effect

Due to the small magnitude and extensive coupling with both the first and third effect, data for the second ('slow') effect is at best poor (Table III). The slow third effect totally obscured the baseline of the second effect at many concentrations causing

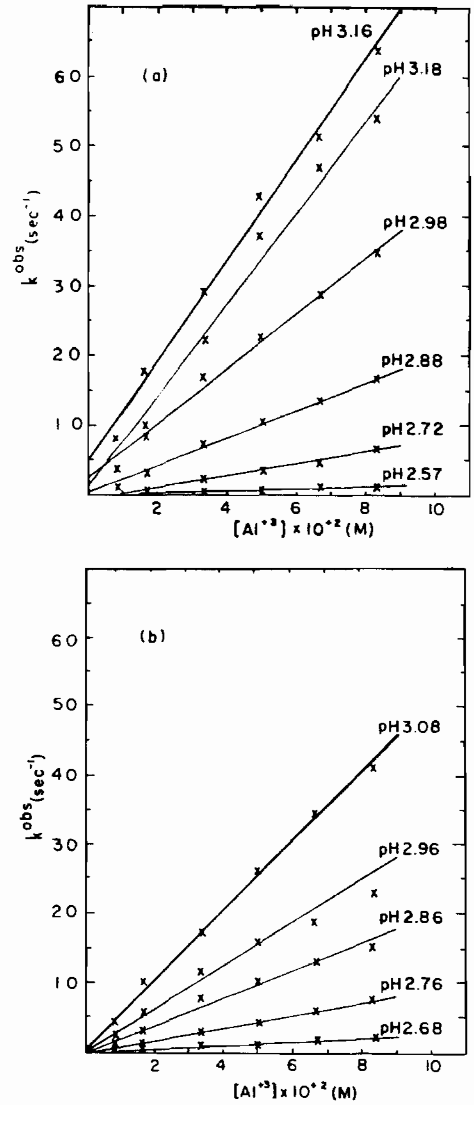

Fig. 2. 'Fast' effect. Observed rate constant *vs.* total initial aluminum(III) concentration at different pH's: [ferron] = 1.45 × 10^{-4} *M*. (a) 'Fast' effect with ClO_4^- as the counter anion; (b) 'fast' effect with Cl^- as the counter anion.

TABLE IV. Observed and Apparent Rate Constants for pH Variation Study at Constant Ferron and Aluminum(III)-Cation Concentrations.

pH	$[\text{Ferron}]_{\text{total}}$ × 10^4 (M)	$[\text{Al}^{+3}]_{\text{total}}$ × 10^2 (M)	$k^{\text{obs}}_{\text{'fast'}}$, ($\text{sec}^{-1}$)	$k^{\text{app}}_{\text{'fast'}}$, ($\text{sec}^{-1}$)^a	$k^{\text{obs}}_{\text{'slow'}}$, ($\text{sec}^{-1}$)
ClO_4^- anion					
2.43	3.1	2.90	0.32(0.04)	0.061	3.05(0.04) × 10^{-2}
2.63	3.1	2.90	0.61(0.09)	0.094	0.11(0.02)
2.83	3.1	2.90	1.2(0.2)	0.15	0.43(0.02)
2.90	3.1	1.45	0.63(0.06)	0.15	0.07(0.05)
2.92	3.1	1.45	1.0(0.1)	0.24	0.10(0.02)
2.94	3.1	1.45	0.83(0.06)	0.19	0.08(0.01)
2.96	3.1	1.45	1.32(0.04)	0.30	0.19(0.01)
3.13	3.1	2.90	3.5(0.1)	0.38	–
3.22	3.1	1.45	4.2(0.5)	0.85	1.3(0.1)
3.33	3.1	2.90	13.7(0.8)	1.4	–
3.43	3.1	2.90	29.9(1.2)	2.9	–
3.53	3.1	1.45	15.6(0.9)	2.9	–
NO_3^- anion					
2.49	6.20	5.81	0.075(0.005)	0.0069	0.015(0.005)
2.69	6.12	5.81	0.112(0.005)	0.0083	0.031(0.005)
2.79	6.12	5.81	0.29(0.01)	0.020	0.06(0.01)
2.99	6.21	5.81	1.14(0.06)	0.067	–
3.19	6.15	5.81	4.96(0.25)	0.27	–
3.39	6.21	5.81	19.2(0.7)	1.0	–
3.49	6.18	5.81	24.2(0.6)	1.3	–
3.49	6.15	5.81	34.2(1.8)	1.8	–
3.49	6.07	5.81	53.3(2.3)	2.8	–
3.59	6.12	5.81	50.6(1.6)	2.8	–
3.79	6.12	5.81	57.8(2.3)	4.7	–
3.89	6.26	5.81	52.8(2.3)	7.6	–
3.99	6.12	5.81	46.4(2.7)	10.4	–

[a] Values obtained by evaluation of eqn. (1) as described in the text.

elimination of these data from consideration because of the high errors involved.

Plots of k^{obs} *versus* total metal concentration (Fig. 3), show a first-order metal dependence and an increasing rate with increasing pH. These trends are the same as those with the 'fast' effect but are not as strong.

No systematic study was made of the third effect so neither the pH or metal dependence is known. The scattered data that was taken gave observed rate constants on the order of 4 × 10^{-3} sec^{-1} with little apparent metal or pH dependence.

pH Variation at Constant Metal Concentration

The results of a pH variation study are listed in Table IV. In this study the concentration of the

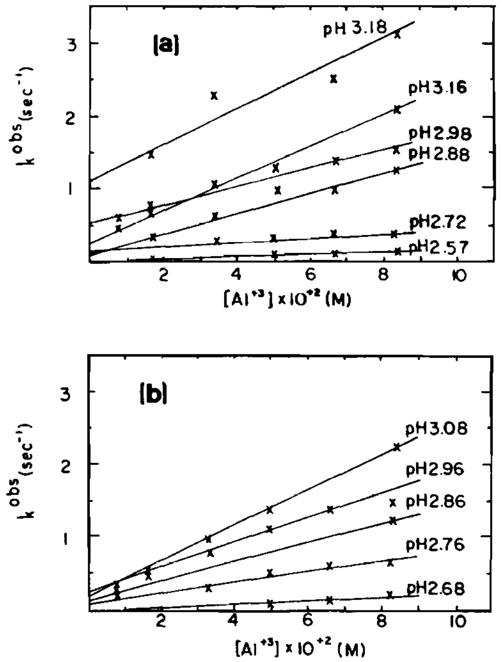

Fig. 3. 'Slow effect'. Observed rate constant *vs.* total initial aluminum(III) concentration at different pHs: [ferron] = 1.45 × 10^{-4} *M* (same solutions as in Fig. 2). (a) 'Slow' effect with ClO_4^- as the counter anion; (b) 'slow' effect with Cl^- as the counter ion.

TABLE V. Observed Rate Constants for an Anion Variation Study.

pH = 2.92
$[\text{Ferron}]_{\text{total}} = 1.45 \times 10^{-4}$ *M*

$[Al^{+3}]_{total}$ × 10^2 (*M*)	0.645	0.967	1.29	
		k^{obs} $(sec^{-1})^a$		
ClO_4^- anion	0.36(0.1)	0.42(0.1)	0.36(0.1)	'fast' effect
	$1.72(0.08) \times 10^{-2}$	$1.9(0.3) \times 10^{-2}$	$2.2(0.1) \times 10^{-2}$	'slow' effect
Cl^- anion	0.31(0.04)	0.24(0.03)	0.31(0.02)	'fast' effect
	$7.9(0.6) \times 10^{-3}$	$1.03(0.03) \times 10^{-2}$	$1.28(0.05) \times 10^{-2}$	'slow' effect
NO_3^- anion	0.32(0.05)	0.32(0.02)	0.36(0.01)	'fast' effect
	$7.7(0.6) \times 10^{-3}$	$1.3(0.9) \times 10^{-2}$	$1.81(0.03) \times 10^{-2}$	'slow' effect

[a] Ref. to Table VI fn. b.

ligand and of the 'freshly prepared' aluminum perchlorate (or nitrate) was held constant. The pH's of the solutions were not corrected for the electrode coating as was done in the metal–pH variation study.

At the lower pH's the observed effect was a composite of two increasing absorbance changes with the second slower effect masking the faster one. With care these effects can be separated, and the resulting k^{obs}'s correspond well to those found with aged solutions when the high error in the pH is considered.

Anion Variation

In this study, (Table V) the metal concentration of 'freshly prepared' aluminum perchlorate, chloride and nitrate were varied over a small range at constant ligand concentration and pH (not corrected for electrode coating).

All runs showed two effects with the slower being the major contributor to the amplitude. The small fast effect showed no metal dependency over the small range used with the value of k^{obs}_{fast}, being about $3.5(0.5) \times 10^{-1}$ sec^{-1} for all three anion systems. The slower second effect showed a linear dependence on total metal concentration with the slope of the k^{obs}_{slow}, *versus* total metal plot being $7.4(0.3) \times 10^{-1}$ M^{-1} sec^{-1} for perchlorate, and $6.7(0.3) \times 10^{-1}$ M^{-1} sec^{-1} for chloride. The corresponding value for nitrate was $1.4(0.1) \times 10^{0}$ M^{-1} sec^{-1} but with a negative intercept. This pronounced difference in the rates between nitrate and the other anions indicates an interaction of nitrate with the reactants of the second effect.

Data Analysis

The simplest kinetics scheme to consider is (*A*)

$$M + L \rightleftharpoons ML \qquad (A)$$

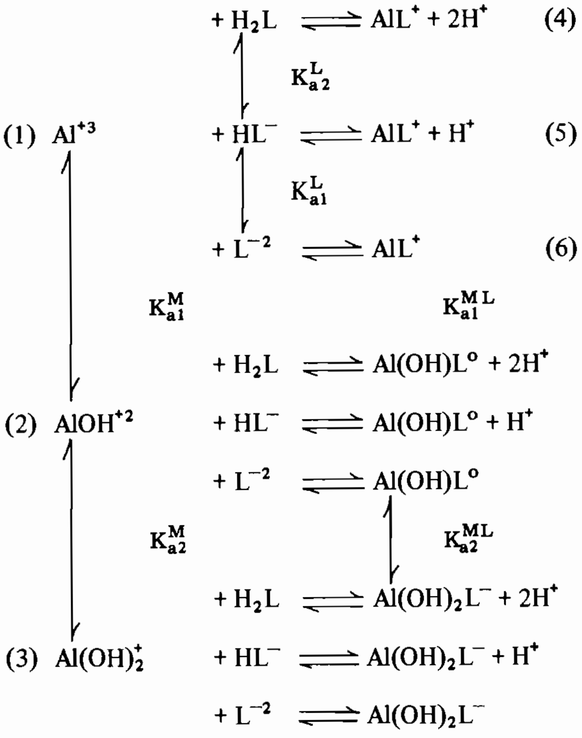

Fig. 4. Complexation of the three monomeric hydrolytic forms of aluminum(III) by the three forms of ferron (H_2L, HL^- and L^{2-}). The individual rate constants are defined as k_{ij} with i being the aluminum species and j the ferron species involved. Thus, k_{24} is the rate constant for the formation of Al(OH)L from $AlOH^{+2}$ and H_2L. The reverse rates are designated by inverting the order; *e.g.*, the reverse rate for k_{24} would be k_{42}.

When M and ML represent the sum of all the possible protolytic species that form from the parent species; *i.e.*, $M \equiv Al^{+3} + AlOH^{+2} + Al(OH)_2^+$, we obtain

TABLE VI. Apparent Rate Constants for the 'Fast' Effect of the Aluminum(III)-Cation–Ferron Reaction.[a]

pH	k_f^{app} (sec^{-1})[b]	k_r^{app} (sec^{-1})
ClO_4^- anion		
2.57	0.088(0.01)	−0.12(0.11)
2.72	0.35(0.01)	−0.7(0.2)
2.88	0.79(0.02)	−0.5(0.3)
2.98	1.40(0.09)	0.9(1.1)
3.16	2.43(0.09)	1.8(1.2)
3.18	2.29(0.09)	−2.2(1.3)
Cl^- anion		
2.68	0.12(0.01)	−0.14(0.09)
2.76	0.41(0.01)	−0.6(0.2)
2.86	0.74(0.03)	−0.1(0.4)
2.96	1.00(0.06)	0.5(0.8)
3.08	1.70(0.03)	−0.03(0.4)

[a]Obtained by fitting data from Table II to eqn. (3). [b]The number in parenthesis for each entry is its associated standard deviation (±sigma).

Fig. 4. In all the experiments the metal is in pseudo-first-order-excess, and the scheme can be analyzed as an approach-to-equilibrium system. The derivation of the expression for k^{obs} from the instantaneous rate equations, using the appropriate hydrolysis equilibrium constants, mass balance equations and expansion around equilibrium, yield [19]

$$k^{obs} = k_f^{app} \frac{\overline{Al}\cdot\overline{H}}{\overline{H}^2 + \overline{H}\cdot K_{a2}^L + K_{a1}^L\cdot K_{a2}^L} + \frac{\overline{H_2L}\cdot\overline{H}}{\overline{H}^2 + \overline{H}\cdot K_{a1}^M + K_{a1}^M K_{a2}^M} + k_r^{app} \quad (1)$$

with $\overline{Al}$, $\overline{H_2L}$, $\overline{H}$ being the concentrations of these specific species at equilibrium.

Concentrations were calculated by means of a Newton–Raphson iteration that generated the equilibrium distribution of all the species present at a given hydrogen ion concentration [19]. Least squares analysis of the k_{fast}^{obs} data from Table II gave the k_f^{app} and k_r^{app} data listed in Table VI. The values of k_r^{app} are not significantly different from zero and due to their high error are included only for completeness.

Since k_f^{app} is the sum of the different reaction pathways, which differ in the degree of protonation of the reactants, its [H]-dependence should give insight into the major pathway involved in the reaction. Figure 5a shows the pH dependence of k_f^{app}. Plotting against $1/[H]^2$ yields a linear plot with a non-negative intercept (Fig. 5b). A linear least squares fit gives a slope of 1.15(0.14) X 10^{-6} M^2 sec^{-1} and intercept of 0.10•(0.17) sec^{-1}.

The data, listed in Table IV, from the constant metal study can be analyzed in a similar manner if the k_r^{app} is eliminated through the use of the overall stability constant for the complex.

$$k_r^{app} = k_f^{app}\{\overline{H}/(K_{11}^{ML}\cdot K_{a1}^L\cdot K_{a2}^L)\} \quad (2)$$

Elimination of k_r^{app} from eqn. (1) gives an analytic expression for k_f^{app} in terms of $\overline{M}$, $\overline{H_2L}$ and $\overline{H}$ which are obtained from an equilibrium distribution calculation. These k_f^{app} are listed in Table IV and give a linear plot as a function of $1/[H]^2$, whose slopes and intercepts are respectively 3.0(0.2) X 10^{-7} M^2 sec^{-1} and 0.2(1.0) X 10^{-1} for perchlorate, 1.08(0.05) X 10^{-7} M^2 sec^{-1} and 4.2(1.9) X 10^{-1} for nitrate. These values are very different from those found from the metal–pH variation study but may be reconciled if the problem of pH is considered. Since there was no quantitative adjustment of the pH in this study the values of the pH's are high. If an arbitrary correction of 0.3 pH units is made to the pH of the perchlorate data, the slope and intercept found upon reanalysis are 1.2(0.1) X 10^{-6} M^2 sec^{-1} and 9.3(1.2) X 10^2 sec^{-1}, in good agreement with the metal–pH variation results.

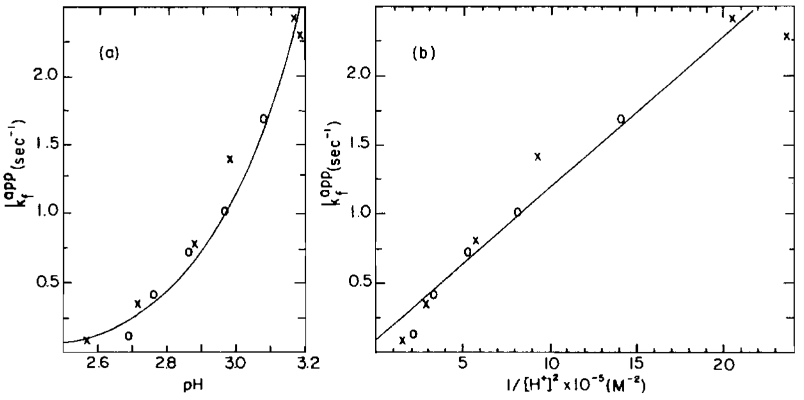

Fig. 5. The hydrogen ion dependence of k_f^{app}: (X) ClO_4^- anion, (o)Cl^- anion. (a) k_f^{app} *vs.* pH; (b) k_f^{app} *vs.* $1/[H^+]^2$.

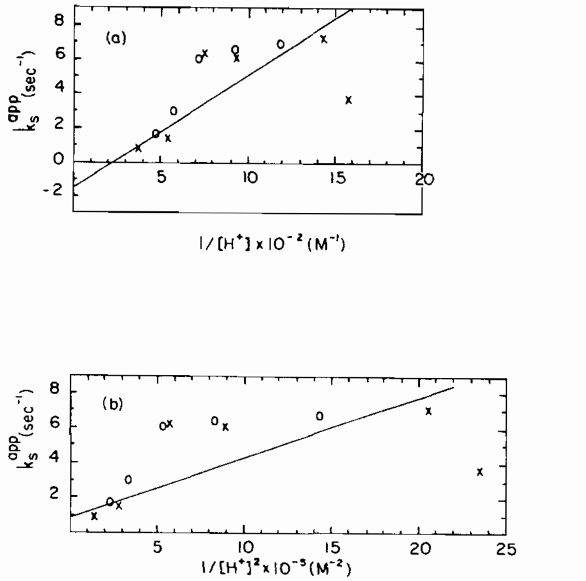

Fig. 6. The inverse hydrogen ion dependence of k_s^{app}: (x) ClO_4^- anion, (o) Cl^- anion. (a) k_s^{app} *vs.* $1/[H^+]$; (b) k_s^{app} *vs.* $1/[H^+]^2$.

TABLE VII. Apparent Rate Constants for the 'Slow' Effect of the Aluminum(III)-Cation–Ferron Reaction.[a]

pH	k_s^{app} $(sec^{-1})^b$	k_b^{app} $(sec^{-1})^c$
ClO_4^- anion		
2.57	0.0089(0.0011)	−0.02(0.04)
2.72	0.015(0.002)	0.1(0.06)
2.88	0.062(0.016)	0.4(0.1)
2.98	0.06(0.01)	0.3(0.2)
3.16	0.071(0.005)	0.24(0.06)
3.18	0.036(0.006)	0.7(0.1)
Cl^- anion		
2.68	0.016(0.001)	−0.06(0.02)
2.76	0.030(0.005)	0.10(0.07)
2.86	0.060(0.002)	−0.03(0.03)
2.96	0.063(0.009)	0.19(0.12)
3.08	0.068(0.010)	0.09(0.1)

[a] Obtained by fitting data from Table III to eqn. (3). [b] The number in parenthesis for each entry is its associated standard deviation (±sigma). [c] Where k_b^{app} is the apparent reverse rate constant for the 'slow' effect.

The slope of the k_f^{app} *versus* $1/[H^+]^2$ plot is of the form

$$\text{slope} = k_{26}K_{a1}^{L}K_{a2}^{L}K_{a1}^{M} + k_{35}K_{a2}^{L}K_{a1}^{M}K_{a2}^{M} \quad (3)$$

with k_{26} and k_{35} corresponding to

$$AlOH^{+2} + L^{-2} \rightleftharpoons Al(OH)L$$

and

$$Al(OH)_2^+ + HL^- \rightleftharpoons Al(OH)_2L^- + H^+$$

respectively. Substitution of the appropriate equilibrium constants gives the expression

$$\text{slope} = 1.5 \times 10^{-6}\ M^2\ sec^{-1} =$$

$$= 3.98 \times 10^{-16}\ k_{26} + 1.17 \times 10^{-13}\ k_{35} \quad (4)$$

with the value of the slope found from the metal–pH variation data.

The 'slow' second effect for the metal–pH variation study has been analyzed in the same manner as the 'fast' effect. The results (given in Table VII) show high scatter when plotted as functions of 1/[H] and $1/[H]^2$ (Fig. 6), but if the best fit line is taken by least squares the slope and intercepts found are for 1/[H]: $6.7(1.6) \times 10^{-5}$ and $-1.4(0.9) \times 10^{-2}$ and for $1/[H]^2$ $3.3(1.1) \times 10^{-8}$ and $9.8(5.2) \times 10^{-3}$.

The preceding analysis was only concerned with explaining the 'fast' effect; consideration of the second effect necessitates inclusion of other processes into the mechanism. Further ligand complexation leads to scheme (*B*)

$$\begin{aligned} &M + L \rightleftharpoons ML \\ &ML + L \rightleftharpoons ML_2 \end{aligned} \quad (B)$$

with M, L, ML, ML_2 again being the sum of all protonated forms of the parent species.

This two-relaxation system however does not adequately explain the observed behavior of the system. An equilibrium distribution calculation for excess aluminum conditions and the pH's used in these studies shows that the relative amount of ML_2 to ML present is only 0.1%. Even if the extinction coefficient of the ML_2 complex were zero at the wavelength used for observation, the conversion of only 0.1% of the ML formed would not account for the 2–5% decrease in absorbance that is observed. Also, since the chromophore of the complex is the coordinated ligand, addition of another ligand to ML should lead to an increase in the extinction coefficient of the complex, rather than the decrease needed to explain the observed absorbance change.

The age of the reacting aluminum solution seems to be a factor in the relative magnitudes of the first two observed effects. This variation may be indicative of the presence of reactive species whose concentrations are different initially from those present when the system adjusts to equilibrium upon aging. At the aluminum concentrations used in these studies there

TABLE VIII. Apparent Forward Rate Constants for the Aluminum(III)-Cation–Ferron Reaction.[a]

pH	$k^{app\,b}_{M+L}$	$k^{app}_{M_2}$	$k^{app}_{M_2+L}$	$k^{app}_{M_2L}$
ClO_4^- anion				
2.57	0.045(0.005)	0.24(0.02)	8.8(0.8) × 10^1	0.02(0.01)
2.72	0.04(0.03)	0.94(0.02)	6.8(0.6) × 10^2	0.17(0.08)
2.88	0.58(0.20)	4.6(0.2)	7.3(4.4) × 10^2	0.42(0.04)
2.98	0.47(0.23)	5.2(0.06)	3.4(0.5) × 10^3	0.78(0.04)
3.16	0.80(0.45)	9.4(0.2)	8.1(1.3) × 10^3	1.05(0.02)
3.18	0.33(0.24)	8.7(0.3)	1.0(0.1) × 10^4	0.99(0.09)
Cl^- anion				
2.68	0.09(0.02)	0.49(0.03)	7.2(4.7) × 10^1	0.6(0.01)
2.76	0.12(0.08)	1.8(0.04)	7.3(2.0) × 10^2	0.28(0.01)
2.86	0.34(0.12)	3.8(0.02)	1.6(0.3) × 10^3	0.44(0.01)
2.96	0.24(0.30)	5.2(0.08)	2.5 × 10^3	0.56(0.01)
3.08	1.5(0.1)	6.9(0.8)	1.8(0.2) × 10^3	0.29(0.12)

[a] Rate obtained by a nonlinear least squares fit to the three relaxation system outlined and derived in Appendix III. [b] The number in parenthesis for each entry is its associated standard deviation (±sigma).

are significant amounts of dimeric, trimeric and polymeric species present. Complexation between ferron (AB) and these species, leading to the ligated dimeric hydroxy bridged complexes shown below, and which are similar to comparable iron(III) complexes [2], can explain the data.

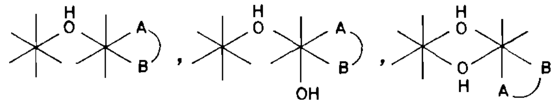

Scheme (*C*) expresses this idea

$$\begin{aligned} M + L &\rightleftharpoons ML \\ 2M &\rightleftharpoons M_2 \\ M_2 + L &\rightleftharpoons M_2L \\ M_2L &\rightleftharpoons ML + M \end{aligned} \qquad (C)$$

If all the forms of the dimeric species present are considered, this mechanism is a five relaxation system which is unmanageable. The problem can be reduced to a more manageable three relaxation system if the reactions involved with the formation of and complexation by the di-μ-hydroxy aluminum species are not considered as being contributory.

The derivation of the relaxation expressions for this mechanism follows standard techniques of relaxation spectrometry [19]. The apparent forward rate constants for all the data from Tables II and III are given in Table VIII.

Discussion

The shortest-lived transient has been assigned to formation of a monocomplex. If the Eigen mechanism is used as a model for the elementary steps in (*A*), the observed rate constant, k_{ij}, is related to the water exchange rate constant for the i^th^ to j^th^ step, $k_{ex}^{species}$ by

$$k_{ij} = K_{OS}^{ij}\, k_{ex}^{species} \qquad (5)$$

where K_{OS}^{ij} is the relevant ion-pair formation constant [21].

Analysis of the 'fast' effect data leads to two kinetically indistinguishable pathways: k_{26}, $AlOH^{+2} + L^{-2}$; and k_{35}, $Al(OH)_2^+ + HL^-$. If in eqn. (4), $3.98 \times 10^{-16}\, M^3\, k_{26} \ll 1.17 \times 10^{-13}\, M^3\, k_{35}$ then

$$k_{35} = 1.28 \times 10^7\, M^{-1}\, sec^{-1} = K_{OS}^{35}\, k_{ex}^{Al(OH)_2} =$$
$$= 0.32\, M^{-1}\, k_{ex}^{Al(OH)_2^+},$$

and

$$k_{ex}^{Al(OH)_2^+} = 4.0(0.4) \times 10^7\, sec^{-1}.$$

Similarly, if the reverse inequality holds then

$$k_{26} = 3.8 \times 10^9\, M^{-1}\, sec^{-1} = K_{OS}^{26}\, k_{ex}^{AlOH^{+2}} =$$
$$= 1.8\, k_{ex}^{AlOH^{+2}}$$

and

$$k_{ex}^{AlOH^{+2}} = 2.1(0.2) \times 10^9 \text{ sec}^{-1}.$$

The value of $k_{ex}^{Al^{+3}}$ has been estimated to be 0.13–0.22 sec^{-1} by Fiat and Connick in an ^{17}O NMR study [8]. Values for $k_{ex}^{AlOH^{+2}}$ in the range 5×10^2 to 5×10^4 sec^{-1} have been reported [8], as a result of kinetics studies analyzed in terms of the Eigen mechanism. In light of these values and that of the corresponding 2×10^3-fold increase in the substitution rate constants of Fe^{+3} and $FeOH^{+2}$, the value of 2×10^9 sec^{-1} for $k^{Al(OH)^{+2}}$ is unreasonable. But if addition of another labilizing OH^- to the metal center is considered to be cumulative then 4×10^7 sec^{-1} for $k^{Al(OH)_2^+}$ is not unreasonable.

For the slow effect, incorporation of dimeric complexing centers into the reaction scheme leads to a model which fits the observed behavior of the reaction. Due to the approximations involved in reducing the computational problem to manageable proportions, the errors in the derived apparent rate constants are large. This constraint limits the resolution of the rate constants and such analysis has been carried out for only two of the four rates.

The rate of constants of the M + L reaction give a straight line when plotted against $1/[H]^2$ with a slope of $3.9(0.8) \times 10^{-7}$ M^2 sec^{-1}, which is similar to the equivalent slope from the simpler mechanism. Substitution of the appropriate stability constants gives the exchange rate constant for the $Al(OH)_2^+$ species as 1.3×10^7 sec^{-1}, consistent with the previous analysis.

The rate constant for the dimer + ferron reaction may be resolved somewhat, with the $1/[H]^2$ plot yielding a reasonably straight line of slope 4.5(0.2) $\times 10^{-3}$. Estimating $K_{a1}^{M_2}$ as being approximately the value for K_{a2}^{M}, gives

$$4.5 \times 10^{-3}\, M \text{ sec}^{-1} = 1.2 \times 10^{-10}\, M^2\, k_{15}^{M_2+L} +$$

$$+ 2.2 \times 10^{-8}\, M^2\, k_{24}^{M_2+L}$$

or

$$2.04 \times 10^5\, M \text{ sec}^{-1} = 5.4 \times 10^{-3}\, k_{24}^{M_2+L}$$

Treatment of this slope in terms of the Eigen model and substituting the appropriate outer sphere equilibrium constant ($K_{OS}^{52} = 1.05 \times 10^{+3}$ M, $K_{OS}^{41} = 9.8$ at $\mu = 1$ M) yields

$$2 \times 10^5\, M^{-1} \text{ sec}^{-1} = 5.7\, M\, k_{ex}^{Al_2} + 9.8\, M\, k_{ex}^{Al_2OH}$$

The exchange rate for $Al_2OH = w_5.AlOH\ Alw_5^{5+}$ ($w = H_2O$) should be between that of Alw_6^{3+} and $AlOHw_6^{2+}$ since the labilizing hydroxide is shared between two metal centers. Therefore an upper limit of about 5×10^4 sec^{-1} may be put on $k_{ex}^{Al_2OH}$. This upper limit then implies that the k_{5d} pathway does not contribute and that

$$2 \times 10^5 = 9.8\, k_{ex}^{Al_2OH}$$

or

$$k_{ex}^{Al_2OH} \cong 2 \times 10^4 \text{ sec}^{-1}.$$

The experimental results show that the apparently 'instantaneous' first phase of the aluminum(III)–ferron interaction actually consists of several discrete steps. The steps have been successfully analyzed in terms of coupled equilibria involving several species. Consequently, the polyphasic nature of the aluminum–ferron interaction at higher pH should also be understood as showing different groups of reaction, rather than differently reacting metal-containing species.

Acknowledgment

We gratefully acknowledge partial support (K.K.) by NIH Research Grant GM 08893 from the Institute of General Medical Sciences, Public Health Service, and from the Gillette Corporation for a Fellowship (J.H.F.).

References

1 M. Eigen and R. G. Wilkins, *Adv. Chem. Ser., 49,* 55 (1965).
2 E. Mentasti, *Inorg. Chem., 18,* 1512 (1979).
3 D. R. Gildea, A. M. Phipps, J. H. Ferguson and K. Kustin, *Inorg. Chem., 16,* 1257 (1977).
4 C. Kalidar, W Knoche and P. Papadopoulos, *Ber. Bunsenges. Phys. Chem., 75,* 106 (1971); *vide* for references to earlier work.
5 F. Secco and M. Venturini, *Inorg. Chem., 14,* 1978 (1975).
6 B. Perlmutter-Hayman and E. Tapuhi, (a) *Inorg. Chem., 16,* 2742 (1977); (b) *ibid., 18,* 875 (1979).
7 C. Baiocchi and E. Mentasti, *Ann. Chim., 69,* 189 (1979).
8 D. Fiat and R. E. Connick, *J. Am. Chem. Soc., 90,* 608 (1968).
9 C. F. Baes and R. E. Mesmer, 'The Hydrolysis of Cations', Wiley-Interscience, New York (1976).
10 R. C. Turner, *Can. J. Chem., 47,* 2521 (1969).
11 R. W. Smith, *Adv. Chem. Ser., 106,* 250 (1971).
12 W. Gessner and M. Winzer, (a) *Z. Anorg. Allg. Chem., 452,* 151 (1979); (b) *ibid.,* p. 157.
13 W. Perl, *J. Appl. Rad. Isotop., 8,* 211 (1960).
14 R. A. Robinson and R. H. Stokes, 'Electrolyte Solutions', Butterworths, London (1959), p. 232.
15 Ref. 9, pp. 22 and 121.
16 R. C. Turner, (a) *Can. J. Chem., 54,* 1910 (1976); (b) *ibid., 54,* 1528 (1976); (c) *ibid., 53,* 2811 (1975).
17 J. Aveston, *J. Chem. Soc.,* 4438 (1965).
18 J. W. Akitt, N. N. Greenwood, B. L. Khandelwal and G. D. Lester, *J. Chem. Soc., Dalton Trans.,* 604 (1972).
19 John H. Ferguson, *Ph.D. Dissertation, Brandeis University* (1979).
20 C. F. Richard, R. L. Gustafson and A. E. Martell, (a) *J. Am. Chem. Soc., 81,* 1033 (1959); (b) R. L. Gustafson and A. E. Martell, *Ann. N.Y. Acad. Sci., 88,* 322 (1960).
21 K. Kustin and J. Swinehart, *Prog. Inorg. Chem., 13,* 107 (1970).